DMD Fast Forward. Published on March 11, 2011 as doi:10.1124/dmd.110.037671

DMD #37671

Identification of Amiodarone Metabolites in Human Bile by Ultra Performance Liquid Chromatography/Quadrupole Time-of-Flight Mass Spectrometry

Pan Deng, Tiangeng You, Xiaoyan Chen, Tao Yuan, Haihua Huang, and Dafang Zhong

Shanghai Institute of Materia Medica, Chinese Academy of Sciences, Shanghai, China (P. D., X. C., T. Y., H. H., D. Z.); and Shanghai East Hospital, Shanghai, China (T. Y.)

Running Title

Amiodarone Metabolites in Human Bile

Corresponding Author: Dafang Zhong
Shanghai Institute of Materia Medica, Chinese Academy of Sciences, 501 Haike Road, Shanghai 201203, China
Phone: 0086-21-50800738
Fax: 0086-21-50800738
Email: dfzhong@mail.shcnc.ac.cn

Number of text pages: 18 (Without Refs)

Number of tables: 2

Number of figures: 7

Number of references: 29

Number of words in the Abstract: 246

Number of words in the Introduction: 255

Number of words in the Discussion: 1630

ABBREVIATIONS: MDEA, mono-*N*-desethylamiodarone; HLM, human liver microsome; UPLC, ultra-performance liquid chromatography; Q-TOF MS, quadrupole time-of-flight mass spectrometer; DDEA, di-*N*-desethylamiodarone; DAA, deaminated amiodarone; 4-MP, 4-methylpyrazole; MDF, mass defect filtering; TMS, tetramethylsilane; DMSO, dimethyl sulfoxide.

ABSTRACT:

Amiodarone is recognized as an effective drug in the treatment of arrhythmias. Previous experiments demonstrated that mono-*N*-desethylamiodarone (MDEA) was the major circulating metabolite in humans. In addition, dealkylation, hydroxylation, and deamination were minor metabolic pathways. The purpose of this study was to identify the metabolites of amiodarone in the bile obtained from patients with T-tube drainage after oral drug administration. Amiodarone metabolism in vitro was also investigated using human liver microsomes (HLMs) and S9 fraction. Ultra performance liquid chromatography/quadrupole time-of-flight mass spectrometry (UPLC-Q/TOF MS) revealed 33 metabolites in human bile, including 22 phase I and 11 phase II metabolites. The major metabolites were MDEA (M7) and ω-carboxylate amiodarone (M12). Metabolite M12 was isolated from human bile and the chemical structure was confirmed using UPLC-Q/TOF MS and ^{1}H NMR. Moreover, the authentic standards of two hydroxylated metabolites, 2-hydroxylamiodarone and 3'-hydroxylamiodarone, were obtained through microbial transformation. Several novel metabolic pathways of amiodarone in human were proposed, including ω-carboxylation, deiodination and glucuronidation. The in vitro study demonstrated that incubation of HLMs with amiodarone did not give rise to any carboxyl metabolites. In contrast, M12 and its metabolites were detected in human liver S9 incubation samples, and the production of these metabolites were inhibited almost completely by 4-methylpyrazole, an inhibitor of alcohol dehydrogenase, suggesting the involvement of alcohol dehydrogenase in the ω-carboxylation of amiodarone. Overall, UPLC-Q/TOF MS analysis leads to the discovery of several novel amiodarone metabolites in human bile, and underscores the importance of bile as an excretion pathway.

Introduction

Amiodarone is a class III antiarrhythmic benzofuran derivative with extensive clinical usage in the treatment of life-threatening ventricular and supraventricular arrhythmias (Naccarelli et al., 2000). It is an amphiphilic compound with high iodine content. Current understanding of the metabolism of amiodarone is incomplete, and only a few studies have been conducted on the human metabolism of amiodarone. Ha et al. (2005) reported that mono-*N*-desethylamiodarone (MDEA) was the major metabolite of amiodarone in human plasma, and that further metabolism of MDEA leads to the formation of 3′-hydroxyl MDEA, di-*N*-desethylamiodarone (DDEA), and deaminated amiodarone (DAA). Moreover, amiodarone and its metabolites could release iodine in vivo (Broekhuysen et al., 1969), which may cause amiodarone-induced thyroid dysfunction during therapy (Martino et al., 1984; Martino et al., 1988; Pitsiavas et al., 1999). However, no deiodinated metabolites have ever been detected in humans. In addition, little is known about the major elimination route of amiodarone, although previous studies suggested that biliary, rather than renal clearance, was the major route of excretion (Broekhuysen et al., 1969; Latini et al., 1984).

The objective of the present study was to investigate the metabolism of amiodarone in human bile using ultra-performance liquid chromatography/quadrupole time-of-flight mass spectrometry (UPLC/Q-TOF MS). Human bile samples were obtained from T-tube drainage of patients suffering from hepatobiliary diseases and arrhythmia. The metabolite profiles of amiodarone in human bile were characterized following oral administration to patients enrolled in the clinical study. Additionally, the formation of the major oxidized metabolite was further investigated in vitro using human liver microsomes (HLMs) and S9 fraction.

Materials and methods

Materials. Amiodarone hydrochloride and 4-methylpyrazole (4-MP) hydrochloride were purchased from Sigma-Aldrich Co. (St. Louis, MO, USA). Pooled human liver microsomes (HLMs) and S9 fraction were purchased from BD Gentest (Woburn, MA, USA). The microbial strain *Cunninghamella blakesleana* AS 3.153 was purchased from Institute of Microbiology, Chinese Academy of Sciences (Beijing, China). All solvents used for UPLC/Q-TOF MS were of HPLC grade (Merck, Darmstadt, Germany). All solvents used for gel chromatography were of analytical grade (Shanghai Chemical Plant, Shanghai, China). Purified water was generated by a Milli-Q Gradient system (Molsheim, France). Silica gel (300–400 mesh), specifically Sephadex LH-20 gel (Amersham Biosciences, Little Chanfolt, UK), was used for column chromatography, and pre-coated silica gel GF254 plates (Qingdao Marine Chemical Plant, Qingdao, China) were used for TLC.

DMD Fast Forward. Published on March 11, 2011 as DOI: 10.1124/dmd.110.037671
This article has not been copyedited and formatted. The final version may differ from this version.

In Vivo Metabolite Profiling. *Subjects and Sample Collection*. Three patients (one male and two females, 66-89 years old) suffering from cardiac arrhythmia, and who had been surgically treated for hepatobiliary diseases, were enrolled in this study after giving informed consent. The clinical study was performed at the Shanghai East Hospital, Shanghai, China, in accordance with the Declaration of Helsinki and was consistent with State Food and Drug Adminastration guidelines for good clinical practice (http://www.chinafdc-law.com/laws/detail_140.html). The study protocol was approved by the hospital ethics committee. After patients had received oral doses of amiodarone hydrochloride tablet (200 mg/day) for the previous 7 days, bile was collected intermittently (about 10 ml) in 1-h intervals for a total of 24 h from their T-tubes. Bile samples were stored at −20°C until analysis.

Bile Sample Preparation and β-glucuronidase Hydrolysis. To a 100 μl aliquot of bile sample was added 200 μl of acetonitrile. After vortex-mixed and centrifuged at 11,000 *g* for 5 min, the supernatant was transferred into a glass tube, evaporated to dryness under a stream of air at 40ºC, and reconstituted in 100 μl of acetonitrile and water (10: 90, v/v). Hydrolysis of glucuronide conjugates was carried out using β-glucuronidase (2000 unit of Type HA-4, Sigma Chemical Co., St. Louis, MO, USA). For enzymatic incubation, a 200 μl aliquot of bile sample was mixed with 200 μl of β-glucuronidase (in 1 M citrate buffer solution at pH 5.0). The incubation was carried out at 37°C for 16 h. The effect of the glucuronidase was studied by comparing the LC-MS peak intensities for compounds of interests before and after the enzymatic incubation. The compounds of interest included glucuronide conjugates and their non-glucuronidated forms (hydrolyzed forms).

UPLC-Q/TOF Mass Spectrometry. Chromatographic separation for metabolite profiling was achieved using an Acquity UPLC system (Waters Corp., Milford, MA, USA) on an Acquity UPLC HSS T3 column (1.8 μm, 2.1 mm × 100 mm, Waters Corp.). The mobile phase was a mixture of (A) 0.05% formic acid in water and (B) 0.05% formic acid in acetonitrile. The gradient elution started from 5% B, increased linearly to 70% B over 15 min, increased linearly to 100% B over the next 2 min, was maintained at 100% B for 1 min, and finally decreased to 5% B to re-equilibrate the column. The column temperature was set at 40°C and the flow rate was 0.4 ml/min. The elute was monitored by UV detection at 265 nm. The MS detection was conducted using a Synapt Q-TOF high-resolution mass spectrometer (Waters Corp., Milford, MA, USA) operated in positive ion electrospray (ES +ve) mode. Nitrogen and argon were employed as the API and collision gas, respectively. Data were acquired from 80–1000 Da using a source temperature of 100°C, a desolvation temperature of 350°C, and cone voltage of 50 V. Data were centroided during acquisition

using an internal reference comprising a 400 ng/ml of leucine enkephalin solution infused at 5 μl/min to generate a reference ion in ES +ve mode at *m/z* 556.2771. Data acquisition was achieved using MS^E, which has two separate scan functions that are programmed with independent collision energies. In this way, a low collision energy scan can be immediately followed by a scan where the collision energy is ramped over a higher range to induce fragmentation of the ions transmitted through Q1. Acquiring data in this manner provided for collection of intact precursor ions as well as fragments.

The mass spectrometer and UPLC system were controlled by MassLynx 4.1 software. Data processing was performed using a MetaboLynx subroutine of the MassLynx software. The mass defect filtering (MDF) for screening metabolites employed a 40 mDa filter between the filter template and the target metabolites. Comparison of fragment ion spectra between the parent compound and metabolites further aided in the identification of metabolite structures and site(s) of modifications in the parent molecule.

Isolation of the Major Metabolite from Human Bile. Semi-preparative HPLC was performed on Shimadzu LC-6AD pumps equipped with a Shimadzu SPD-20A UV detector (248 nm). Human bile samples (2000 ml) were first extracted three times by EtOAc. The EtOAc soluble fraction was subjected to silica gel chromatography in a gradient (CH_2Cl_2/MeOH/Et_2NH, 15/1/0.01 to 0/1/0.01, v/v) to yield five fractions (A–E). Fraction E was separated over a Sephadex LH-20 column eluted with MeOH to obtain six subfractions (E1–E6). Subfraction E3 was purified by semi-preparative HPLC using a YMC-Pack ODS-A column (250 mm × 10 mm, S-5 μm, 12 nm) and a mobile phase consisting of (A) methanol and (B) aqueous 5% acetic acid plus 5% Et_2NH. The isocratic elution used 75% A at a flow rate of 3 ml/min to isolate the major metabolite in human bile.

Microbial Transformation and Isolation of Hydroxylated Metabolites. Frozen microbial stock culture of *Cunninghamella blakesleana* AS 3.153 was incubated in 250-ml flasks containing potato dextrose agar (Aoboxing, Beijing, China) at 28°C for 7 days in a rotary shaker set to 200 rpm. At the end of this period, the seed culture (10 ml) was inoculated into 250-ml flasks containing 50 ml of biotransformation medium, which consisted of dextrose (2.0 g), yeast extract (0.5 g), peptone (0.5 g), NaCl (0.5 g), and K_2HPO_4 (0.5 g) in 100 ml of distilled water. After incubation at 28°C and 200 rpm for 24 h, a 0.5 ml portion from the first-stage culture was used to inoculate a second-stage culture that was incubated for 24 h before the addition of amiodarone in methanol (9:1, v:v) for a final concentration of 640 μg/ml. The methanol content in the transformation system was less than 2%. After 3 days, the fermentation was harvested, and the cells were removed by centrifugation (2,000 *g*, 10 min).

DMD Fast Forward. Published on March 11, 2011 as DOI: 10.1124/dmd.110.037671
This article has not been copyedited and formatted. The final version may differ from this version.

The supernatant (1500 ml) was extracted three times with EtOAc (1500 ml). The EtOAc soluble fraction was subjected to silica gel chromatography in a gradient (CH_2Cl_2/MeOH/Et_2NH, 15/1/0.01 to 0/1/0.01, v/v) to yield three fractions (A–C). Fraction B was purified by semi-preparative HPLC (A: MeOH, B: H_2O with 5% acetic acid and 5% Et_2NH, A: B = 80: 20, 3 ml/min) to isolate the hydroxylated metabolites.

The structures of the three standard compounds were characterized by high resolution Q-TOF mass spectrometry and NMR. The NMR spectra were recorded on a Bruker AM-400 (Newark, DE, USA) or a Varian INOVA 600 spectrometer (Palo Alto, CA, USA) using tetramethylsilane (TMS) as an internal standard. All compounds were dissolved in deuterated methanol. Chemical shifts are expressed as parts per million relative to TMS.

In Vitro Metabolite Profiling. All incubations were performed at 37°C in a water bath. A stock solution of amiodarone was prepared in dimethyl sulfoxide (DMSO). The final concentration of DMSO in the incubation was 0.1% (v/v). The HLMs and human liver S9 fraction were carefully thawed on ice prior to the experiment. Amiodarone (50 μM) was mixed with each subcellular fractions (the concentrations of microsomal protein are 1.0 mg /ml for HLM, and 2.0 mg/ml for human liver S9) in 100 mM potassium phosphate buffer (pH 7.4). The total incubation volume was 200 μl. After 3 min of preincubation at 37°C, the incubation reactions were initiated by the addition of NADPH (2.0 mM). After 60 min incubation, the reactions were terminated with an equal volume of ice-cold acetonitrile. To determine the enzymatic pathways involved, separate incubations with human liver S9 were performed in the presence of 4-MP at the final concentration of 5 μM (Sohlenius-Sternbeck et al., 2000; Chmela et al., 2001). Control samples containing no NADPH or substrates were included. Each of the incubations was performed in duplicate. The samples were analyzed using UPLC/Q-TOF MS.

Results

UPLC-Q/TOF MS Analysis of Amiodarone. To identify amiodarone metabolites, the chromatographic and MS fragmentation behaviors of the parent compound were first investigated. The retention time of amiodarone was 18.0 min under the chromatographic conditions employed. In positive scan mode, amiodarone formed a protonated molecule $[M + H]^+$ at *m/z* 646.029. Fig. 1A shows the product ion spectrum of amiodarone under the high collision energy scan. On the basis of the high resolution mass spectral information, a tentative pathway for the formation of the most informative fragment ions of amiodarone is proposed in Fig. 1B. The fragments of amiodarone were formed predominantly by the cleavage of alkyl C-O bond, loss of the 5-keto substituent of the benzofuran moiety, and cleavage of the

DMD Fast Forward. Published on March 11, 2011 as DOI: 10.1124/dmd.110.037671
This article has not been copyedited and formatted. The final version may differ from this version.

C-N bond. Product ions at *m/z* 372.831, 276.082, 247.078, 245.956, 217.926, 201.094, 119.021, and 100.113 (100% abundance) were observed. Detection of these ions in the high collision energy mass spectra of metabolites indicated either the unmodified benzofuran structure (*m/z* 201.094), hydroxybenzaldehyde moiety (*m/z* 372.830 and 245.956) or the unchanged triethylamine (*m/z* 100.113). According to this fragment pattern, the structure of amiodarone was divided into three parts, A, B, and C (Fig. 1B). The high collision energy mass spectra and chromatographic behaviors of detected metabolites were compared with those of the parent compound and available authentic standards to characterize the structural modification.

Amiodarone Metabolites in Human Bile. As shown in Fig. 2A, thirty-three metabolites of amiodarone were detected in human bile samples. Table 1 lists the detailed information of these metabolites, including the retention times, proposed elemental compositions, and the characteristic fragment ions. The structures of metabolites were characterized by mass spectral fragmentation patterns or confirmed by comparison of chromatographic retention times and mass spectra with available reference standards. Proposed structures of the detected metabolites are shown in Fig. 3.

Parent drug M0. A chromatographic peak at 18.0 min was detected with an elemental composition of $C_{25}H_{29}I_2NO_3$, and a protonated molecular weight of 646.032. The retention time and mass spectral fragmentation patterns were identical to the parent drug, amiodarone, indicating that this component was unmetabolized amiodarone, designated as M0.

Metabolite M1. Metabolite M1 had a retention time of 16.2 min, exhibited a protonated molecule at *m/z* 492.104, and the elemental composition was $C_{23}H_{26}INO_3$, suggesting the loss of C_2H_3I from amiodarone. M1 was consequently proposed as a deiodinated metabolite of *N*-desethylated amiodarone. The absence of the fragment ion at *m/z* 100.113 was consistent with modification on the triethylamine moiety.

Metabolite M2. Metabolite M2 was eluted at 13.1 min. It had a protonated molecular weight of 508.099, and accurate mass measurement revealed the chemical formula $C_{23}H_{26}INO_4$, suggesting monohydroxylation of molecule M1. At low collision energy scan, the fragment ions at *m/z* 437.024 and 419.017 were observed, which were resulted from the cleavage of O-C_{14} bond (–71.075 Da, loss of C_4H_9N) and further loss of water (–18.007 Da), indicating hydroxylation was occurred on the *n*-butyl side chain.

Metabolite M3. Metabolite M3 was eluted at 16.3 min with a protonated molecular weight of 546.927. The elemental composition of the metabolite was $C_{19}H_{16}I_2O_3$, suggesting the loss of $C_6H_{13}N$ from the parent compound. The major fragment ion at *m/z* 372.858 was the same as that of the parent drug, while the

DMD Fast Forward. Published on March 11, 2011 as DOI: 10.1124/dmd.110.037671
This article has not been copyedited and formatted. The final version may differ from this version.

fragment ion at *m/z* 100.113 was absent, indicating the loss of the triethylamine moiety. M3 was thus identified as the *O*-dealkylated metabolite of amiodarone resulting from removal of the triethylamine moiety.

Metabolite M4. Metabolite M4 had a retention time of 13.3 min, exhibited a protonated molecule at *m/z* 550.109, and a derived formula of $C_{25}H_{28}INO_5$, suggesting the addition of two oxygen atoms and loss of two hydrogen atoms from deiodinated-amiodarone. High collision energy analysis revealed product ions at 276.070 and 100.113 that were the same as those of the parent drug, indicating benzofuran and triethylamine moieties were intact. Metabolite M4 was tentatively identified as deiodinated-amiodarone with ω-oxidation of the *n*-butyl side chain to a carboxylic acid.

Metabolite M5. Metabolite M5 was eluted at 21.5 min with a protonated molecular weight of 590.953. The elemental composition of the metabolite was $C_{21}H_{20}I_2O_4$, consistent with deamination and hydroxylation of amiodarone. Cleavage of the O-C_{14} bond (–44.023 Da, loss of C_2H_4O) produced the fragment ion at *m/z* 546.930, indicating that hydroxylation occurred in part C. The fragment ions at *m/z* 372.818, 217.927, 201.0913, 119.013 and 91.018 originated from intact parts A and B. Therefore, M5 was proposed to be the oxidative deaminated amiodarone (DAA) identified previously in human plasma (Ha et al., 2005).

Metabolite M6. Metabolites M6-1 and M6-2 were eluted at 14.4 and 18.6 min, respectively, and both displayed a protonated molecule at *m/z* 606.948. Accurate mass measurement showed that the chemical formula of both was $C_{21}H_{20}I_2O_5$, suggesting the addition of two oxygens and loss of C_4H_9N from amiodarone. The major fragment ion at *m/z* 372.858 was the same as that of the parent drug and *m/z* 100.113 fragment was absent, indicating modifications of parts A and C. Other fragment ions included *m/z* 562.924 (–44.024 Da, loss of C_2H_4O) and its dehydrated form at *m/z* 544.915 (562.924 – H_2O) indicating M6-1 and M6-2 were hydroxylation metabolites of M5. Considering the readily loss of water, the sites of hydroxylation for M6-1 and M6-2 were proposed to be on the *n*-butyl side chain.

Metabolite M7. Metabolite M7, eluted at 17.0 min, had a protonated molecular weight of 618.000, which is 28.031 Da lower than the parent drug. The elemental composition of the metabolite was $C_{23}H_{25}I_2NO_3$, indicating the loss of C_2H_4 from the parent molecule. This metabolite contained fragment ions at *m/z* 372.858 and 201.090, indicating that part A and B were intact. The absence of the fragment at *m/z* 100.113 suggested that M7 was *N*-desethylated amiodarone. It was shown to be one of the major metabolites in human bile on the basis of the chromatographic peak area.

DMD Fast Forward. Published on March 11, 2011 as DOI: 10.1124/dmd.110.037671
This article has not been copyedited and formatted. The final version may differ from this version.

Metabolite M8. The protonated molecular weight of M8 was 633.995, which is 12.036 Da less than the protonated parent drug. Its elemental composition was $C_{23}H_{25}I_2NO_4$, indicating the loss of C_2H_4 and the introduction of an oxygen atom into the parent molecule. Five peaks with a protonated ion at *m/z* 633.995 were detected at 13.5 (M8-1), 13.7 (M8-2), 14.0 (M8-3), 14.4 (M8-4), and 14.7 min (M8-5) (Fig. 2B). The fragment at *m/z* 100.113 was absent for these five metabolites, indicating that part C was modified. The fragment at *m/z* 372.820 suggested that the site of hydroxylation was not on part B. These metabolites were proposed to be monohydroxylated metabolites of M7. Moreover, the fragments of M8-2, M8-3 and M8-4 all included the ions at *m/z* 562.922 and 544.908, which were the same as those for M6, suggesting the site of hydroxylation was on *n*-butyl chain.

Metabolite M9. Metabolite M9 was eluted at 13.4 min and possessed a protonated molecular weight of 647.974. The elemental composition of M9 was $C_{23}H_{23}I_2NO_5$, indicating the addition of two oxygen atoms and the loss of two hydrogen atoms from amiodarone to form an *N*-desethyl metabolite of carboxylamiodarone.

Metabolite M10. Metabolites M10-1 and M10-2 eluted at 11.6 and 12.0 min, respectively, and yielded a protonated molecule at *m/z* 649.990. Accurate mass measurement demonstrated that the chemical formula was $C_{23}H_{25}I_2NO_5$, indicating the addition of two oxygen atoms to *N*-desethylated amiodarone. The high energy mass spectrum of M10-1 and M10-2 revealed a characteristic fragment ion at *m/z* 372.823, and several fragment ions originated from part B were also observed at *m/z* 245.923, 217.928, 119.016 and 91.020. However, the mass spectrometry data did not reveal the site of di-hydroxylation. M10-1 and M10-2 were proposed to be mono-hydroxylated metabolites of M8.

Metabolite M11. Metabolite M11 had a protonated molecular weight of 662.026, 15.993 Da higher than that of protonated amiodarone. The elemental composition of the metabolite was $C_{25}H_{29}I_2NO_4$, indicating that an oxygen atom had been introduced into the parent drug. Five chromatographic peaks at 14.3 (M11-1), 14.5 (M11-2), 14.9 (M11-3), 15.3 (M11-4), and 15.5 min (M11-5), with a molecular ion at *m/z* 662.026, were detected (Fig. 2C). The high energy mass spectra of M11-1, M11-2 and M11-5 revealed fragment ions at *m/z* 372.858 and 100.113, indicating that parts B and C were intact, but that hydroxylation occurred on part A.

To pinpoint the site of hydroxylation, metabolites M11-2 and M11-5 were isolated from microbial incubations as described under *Materials and Methods.* The fragmentation patterns and HPLC retention times of the isolated metabolites from in vitro incubations were identical to those detected in human bile.

DMD Fast Forward. Published on March 11, 2011 as DOI: 10.1124/dmd.110.037671
This article has not been copyedited and formatted. The final version may differ from this version.

Proton chemical shifts for metabolites are summarized in Table 2. Comparing the ^{1}H one-dimensional spectra of M11-2 and amiodarone indicated that aromatic ring proton signals in part A were unchanged, but that the *n*-butyl side chain in M11-2 might have been hydroxylated. An oxygenated methine signal at δ_H 3.69 (m, 1H) and a doublet methyl signal at δ_H 1.15 (d, J = 7.2 Hz, 1H) indicated that the hydroxyl was attached to C-3′ (δ_C 66.4). The HMBC correlations (Fig. 4) from H_3-4′, H_2-1′, and H_2-2′ to C-3′, and from H-3′ to C-1′, C-2′, and C-4′ supported the above assignment. M11-2 was accordingly confirmed to be 3′-hydroxylamiodarone. In the ^{1}H NMR spectrum of M11-5, a typical ABX proton coupling system of an aromatic ring at δ_H 6.94 (d, J = 1.7 Hz, 1H), 6.78 (dd, J = 8.5, 1.7 Hz, 1H), and 7.23 (d, J = 8.5 Hz, 1H) indicated the presence of a tri-substituted phenyl ring, and the site of hydroxylation was narrowed to position C-2 or C-3. The HSQC spectrum allowed the assignment of all protons to their bonding carbons. The hydroxylation site remained ambiguous following detailed analysis of the HMBC spectrum, however. Fortunately, the relative upfield chemical shift of C-1 at δ_C 97.2 implied that the hydroxyl group in M11-5 was attached to C-2, which was caused by the electron-donating effect of the oxygen. Metabolite M11-5 was, therefore, identified as 2-hydroxylamiodarone. The hydroxylation site for M11-1 was tentatively proposed at C-4', which led to the formation of ω-hydroxylamiodarone.

Metabolite M12. M12 was the most abundant metabolite in human bile on the basis of the chromatographic peak area. It was eluted at 14.2 min with a protonated molecular weight of 676.006, 29.974 Da higher than the parent drug. The elemental composition of the metabolite was $C_{25}H_{27}I_2NO_5$, suggesting the addition of two oxygen atoms and the loss of two hydrogen atoms from amiodarone. The high energy mass spectrum of M12 gave fragment ions at *m/z* 372.823, 245.926, 217.925 and 100.122 that originated from intact parts B and C, suggesting that part A has been oxidized. The ^{1}H NMR data were obtained for M12 isolated from human bile. Compared to the spectrum of the parent compound (Fig. 5), two methylene proton signals at δ_H 4.29 (t, J = 6.1 Hz, 2H) and 3.36 (t, J = 6.1 Hz, 2H), and two *N*-ethyl signals at δ_H 3.04 (q, J = 6.9 Hz, 4H) and 1.25 (t, J = 6.9 Hz, 6H) were observed, supporting the idea that part C was intact. In addition, the signals of aromatic protons in M12 were in the same range as those of the parent molecule, suggesting that the two aromatic rings in parts A and B were unmodified. Taken together, these data indicated that the *n*-butyl side chain was the site of modification for M12. Further analysis of the ^{1}H NMR spectrum revealed that the proton signals of CH_2-2′ (δ_H 2.06, m, 2H) and CH_2-3′ (δ_H 2.21, m, 2H) were shifted downfield, and that the C-4′ methyl signal of the parent compound disappeared, indicating the presence of an electron-withdrawing group in C-4′. The structure of M12 was thus determined to be

4′-carboxylamiodarone.

Metabolite M13. Metabolite M13, eluted at 11.9 min, had a protonated molecular weight of 726.141 and a derived formula of $C_{31}H_{36}INO_{11}$. High collision energy analysis revealed a characteristic product ion at 550.112 that was due to a neutral loss of 176.027 Da from protonated M13, suggesting that this metabolite was a glucuronide of M4. The position of the glucuronic acid was not determined.

Metabolite M14. Metabolite M14 was eluted at 18.1 min and had a protonated molecular weight of 766.985. The elemental composition of the metabolite was $C_{27}H_{28}I_2O_{10}$, consistent with the deamination, hydroxylation, and glucuronide conjugation. The fragment ion at *m/z* 590.954 corresponded to a neutral loss of 176.033 Da, and the other characteristic fragment at *m/z* 546.930 resulted from further cleavage of the O-C_{14} bond (–44.024 Da, loss of C_2H_4O). This was the same bond cleaved in DAA (M5), indicating that M14 was the glucuronide conjugated metabolite of M5.

Metabolite M15. Metabolites M15-1 and M15-2 were eluted at 12.2 and 19.6 min, respectively, and had a precursor ion at *m/z* 810.027, 176.032 Da larger than M8 (*m/z* 633.995). Accurate mass measurement demonstrated the chemical formula to be $C_{29}H_{33}I_2NO_{10}$, suggesting that M15-1 and M15-2 were glucuronide conjugates of M8 (*m/z* 633.989, $C_{23}H_{25}I_2NO_4$). The fragment at *m/z* 633.998, observed for both M15-1 and M15-2, was formed by neutral loss of 176.036 Da. Metabolite M15-1 produced fragment ions at *m/z* 562.931 and 544.912, which were the same as those for M6. Therefore, the site of hydroxylation for M15-1 was proposed to be on the *n*-butyl side chain. The major fragment ion for M15-2 was *m/z* 372.824, indicating the site of modification was not on part B.

Metabolite M16. Metabolite M16 was eluted at 16.3 min and had a protonated molecular weight of 822.064. The elemental composition of this metabolite was $C_{31}H_{37}I_2NO_9$, corresponding to the glucuronide conjugate of amiodarone. The major fragment ion at *m/z* 646.024 was due to a neutral loss of 176.037 Da. M16 was, therefore, proposed to be a glucuronide of amiodarone, and the site of conjugation was tentatively assigned at the tertiary amine group.

Metabolite M17. Metabolite M17 was eluted at 12.1 min, and had a protonated molecular weight of 824.007, 176.032 Da larger than M9 (*m/z* 647.974). The elemental composition of the metabolite was $C_{29}H_{31}I_2NO_{11}$. High collision energy scan of M17 produced a fragment ion at *m/z* 647.980 resulting from a loss of the neutral glucuronic acid moiety (176.032 Da), indicating the presence of a glucuronide moiety. M17 was proposed to be a glucuronide of M9. The site of conjugation was not established.

Metabolite M18. Metabolites M18-1, M18-2 and M18-3 were eluted at 12.6, 12.8, and 13.0 min,

DMD Fast Forward. Published on March 11, 2011 as DOI: 10.1124/dmd.110.037671
This article has not been copyedited and formatted. The final version may differ from this version.

respectively (Fig. 2D), and had a precursor ion at *m/z* 838.059, 176.032 Da larger than M11 (*m/z* 662.026). Under high collision energy scan, M18-1, M18-2 and M18-3 showed the same major fragment ion at *m/z* 662.027 due to neutral 176.023-Da loss. The remaining fragments at *m/z* 372.825 and 100.113 suggested an unchanged part B and C. Therefore, M18-1, M18-2 and M18-3 were tentatively identified as the glucuronides of the hydroxyl-amiodarone with hydroxylation in part A. After *β*-glucuronidase hydrolysis, the intensity of the peaks corresponding to hydroxylated metabolites of M11-1, M11-2 and M11-5 all increased significantly. Therefore, metabolites M18-1, M18-2 and M18-3 could have been produced by hydroxylation of amiodarone at C-4', C-3' or C-2 followed by the glucuronide conjugation.

Metabolite M19. Metabolite M19-1 and M19-2 were eluted at 12.4 and 12.9 min, respectively. They showed a precursor ion at *m/z* 852.038 and derived elemental composition of $C_{31}H_{35}I_2NO_{11}$. The major fragment ion at *m/z* 676.009 indicated a neutral loss of 176.026 Da, suggesting that M19-1 and M19-2 were glucuronide conjugates of M12; however, the sites of conjugation were not established by the mass spectral data.

Metabolism of Amiodarone in Vitro in Human Liver Microsomes and Human Liver S9. Incubations of amiodarone in HLMs and human liver S9 were performed to determine the hepatic contribution to the overall disposition of this drug. As shown in Fig. 6, compared with the control sample, eighteen oxidized metabolites of amiodarone were detected in HLM incubations. Besides those identified in human bile (M1, M3, M6, M7, M8, M10, and M11), deiodinated-amiodarone (M21, *m/z* 520.138) and *N*-oxide metabolite (M11-6, *m/z* 662.021) were detected. Following incubation with the human liver S9 fraction, several carboxylic acid metabolites were detected aside from those observed in HLMs, including M4, M9 and M12 (Fig. 7). The amiodarone metabolite profiles in HLMs and S9 were different to the profiles observed in human bile. As indicated by LC/UV detection, *N*-desethylamiodarone (M7) was the only principal species found in either HLMs and human liver S9 incubation, while other metabolites were all detected at much lower levels.

Importantly, 4'-carboxylamiodarone (M12) was not detected in the incubations of amiodarone with HLMs, and it was a minor metabolite in human liver S9 incubation in the presence of NADPH (Fig. 7). In another experiment, the human liver S9 was preincubated with 5 μM 4-MP for 10 min before the addition of 50 μM amiodarone and further incubation for 60 min. This resulted in potent inhibition of the formation of 4'-carboxylamidaorne, and the amount of 4'-carboxylamidaorne produced was approximately 10-fold lower in human liver S9 incubations treated with 4-MP than in control samples without 4-MP as

determined from the LC/MS.

Discussion

In general, studies of drug metabolites in human subjects focus on blood, urine, and feces; however, drugs that have high molecular weights are often excreted in the bile. The threshold molecular weight of drugs and metabolites that are preferentially excreted into human bile ranges from 500−600 Da (Ghibellini et al., 2006). Biliary elimination of compounds can significantly influence their systemic or hepatic exposure and pharmacological effects. Amiodarone was speculated to be excreted primarily by hepatobiliary route because of its relative large molecular weight. Indeed, hepatobiliary elimination was supported by the fact that less than 0.5% of the dose was excreted in the urine (Anastasiou-Nana et al., 1982). Feces has been traditionally used to estimate the drug and metabolites excreted via bile in humans (Ghibellini et al., 2006). However, unstable metabolites, such as glucuronides that could be hydrolyzed along the intestine, cannot be characterized properly using this method. Therefore, investigations of amiodarone metabolites in human bile allow for direct identification of metabolites, including intact glucuronides.

In the present study, human bile samples were obtained in T-tube drainage from arrhythmia patients taking amiodarone. The samples were analyzed using the UPLC/Q-TOF MS method, and a total of 33 metabolites, including 22 phase I and 11 phase II metabolites, were detected in the bile extracts. The chemical structures of the metabolites were characterized by their accurate mass, mass spectral fragmentation patterns, and by comparison to reference standards. In particular, 4′-carboxylamiodarone (M12), a major metabolite, was isolated from human bile, and two hydroxylated metabolites, M11-2 (3′-hydroxylamiodarone) and M11-5 (2-hydroxylamiodarone), were obtained through microbial transformation.

Previous investigations of amiodarone metabolism in humans revealed that MDEA was the major metabolite in human plasma (Flanagan et al., 1982) and tissues (Storey et al., 1983; Berdeaux et al., 1984). Given the known pharmacological activity of this metabolite, and the high plasma and tissue concentrations in patients treated with chronic amiodarone therapy, MDEA may be considered as an independent drug. In mammals, MDEA could be transformed to 3’-hydroxyl MDEA both in vivo and in vitro (Ha et al., 1996; Ha et al., 2001a; Ha et al., 2001b; Ha et al., 2005), and 3’-hydroxylation was regarded as a primary metabolite of MDEA in humans (Ha et al., 2005). Further dealkylation and deamination of MDEA could result in low amounts of di-*N*-desethylamiodarone (DDEA) and DAA in human plasma (Freedman and

Somberg, 1991; Ha et al., 2005). In human urine, only negligible amount of amiodarone and MDEA were detectable after oral drug dosing (Harris et al., 1983). In the present study, characterization of metabolites in human bile revealed that amiodarone was extensively metabolized before excretion into bile. Metabolite M7 (MDEA) was identified as one of the major metabolites in human bile, as it is in human plasma. Subsequent oxidation of MDEA lead to several mono- and di-hydroxyl metabolites (M8 and M10), and oxidative deamination resulted in the formation of DAA (M5). However, neither DDEA nor its conjugated metabolites were detected in human bile sample.

On the basis of the chromatographic peak area, the other major route of metabolism was identified as ω-oxidation and the formation of 4'-carboxylamiodarone (M12), and the content of M12 in human bile was estimated to be approximately 3-fold higher than that of the parent drug. Considering that the ionization efficiency for metabolites and the parent drug may be different, the ionization efficiency of M12 and amiodarone were compared using standard compound solutions, and they demonstrated slight differences in ionization efficiency at the same concentration, with the MS response of M12 a little lower than that of amiodarone. This supported the conclusion that carboxylation represented a major metabolic pathway of amiodarone in humans. It has been reported previously that certain compounds with alkyl side chains can be metabolized to carboxylic acids (Harvey, 1989; Samara et al., 1990; Rucker et al., 1992; Sohlenius-Sternbeck et al., 2000), and the formation of these metabolites generally involves two steps, initial ω-hydroxylation of the alkyl side chains by cytochrome P450s, and further oxidation of the ω-hydroxylated intermediates to ω-carboxylic acid metabolites catalyzed by cytosolic alcohol dehydrogenase (Chmela et al., 2001; Walsh et al., 2002). Therefore, a possible mechanism for the formation of 4'-carboxylamiodarone could involve oxidation of the *n*-butyl side chain of amiodarone by cytochrome P450s to the ω-hydroxyl intermediate, followed by oxidation by alcohol dehydrogenase to produce M12. In vitro experiments carried out using HLMs and human liver S9 revealed five hydroxylated metabolites (M11), which were the same as those detected in human bile, whereas M12 could only be detected in incubations with liver S9 fraction. This observation suggested the presence of a liver cytosolic enzyme involved in the formation of M12. In order to demonstrate the involvement of alcohol dehydrogenase in the metabolism of amiodarone, 4-MP, an inhibitor of alcohol dehydrogenase, was preincubated with human liver S9, and the result showed that 4-MP almost completely inhibited the formation of metabolite M12. This finding supported the hypothesis that the second step in the formation of M12 is catalyzed by alcohol dehydrogenase. Among the five mono-hydroxyl metabolites detected in vivo and vitro, the retention time of

DMD Fast Forward. Published on March 11, 2011 as DOI: 10.1124/dmd.110.037671
This article has not been copyedited and formatted. The final version may differ from this version.

M11-1 was the shortest (14.3 min), together with the mass spectral data, the hydroxylation site of M11-1 was proposed to be on the *n*-butyl side chain rather than benzylic carbons. Steric hindrance around the heme FeO^{3+} in cytochrome P450 enzymes limits hydroxylation of sterically hindered carbons, while encourages hydroxylation at the terminal (ω) and penultimate (ω − 1) positions of aliphatic chains (Nassar et al., 2009), M11-1 was therefore tentatively identified as ω-hydroxylamiodarone. Further studies to prove the presence of ω-hydroxylamiodarone are currently underway. In addition, greater insight into the cytochrome P450 enzymes and transporters involved in the formation and elimination of M12 might explain the wide variability of amiodarone pharmacokinetics in humans.

Although the drug metabolites of toxicological concern usually are those circulating in plasma at greater than 10 percent of parent systemic exposure, other metabolites also can elicit safety concern. For example, a metabolite that predominantly excreted into bile may result in bile duct toxicity (February, 2008 FDA Guidance for Industry, Safety Testing of Drug Metabolites. Pharmacology and Toxicology; http://www.fda.gov/cder/guidance/). Therefore, further investigation is needed to understand the importance of metabolite M12 from safety perspective.

Amiodarone contains approximately 37% iodine by weight, and the maintenance daily dose of the drug is 200 to 600 mg. However, the recommended daily intake of iodine is only 150 μg (Shiraishi et al., 2006). Excess iodine released from the parent drug and its metabolites may contribute to the amiodarone-induced thyroid dysfunction, which is a common adverse effect of this drug (Bogazzi et al., 2001). However, the deiodination of amiodarone is still unclear and is a topic of considerable debate. A previous study proposed that deiodination was one of the metabolic pathways of amiodarone in humans (Freedman and Somberg, 1991), and Young et al. (Young and Mehendale, 1986) reported that MDEA could be di-deiodinated in rabbit liver microsomes. However, others claimed that no deiodinated metabolites could be found in vivo and in vitro (Ha et al., 2001a; Ha et al., 2005). Using UPLC-Q/TOF MS as an analytical tool, we observed several ions that could be related to the presence of deiodinated metabolites in human bile (M1, M2, M4, and M13) and in vitro (M1, M2, M4, and M21). Although deiodination is a minor metabolic pathway of amiodarone in humans, attentions should be paid to the impact of relative high amount of iodine released from amiodarone on human health during chronic drug treatment.

Glucuronide conjugation was another metabolic pathway of amiodarone identified in human bile. It was reported that amiodarone could undergo extensive enterohepatic circulation (Freedman and Somberg, 1991; Roden, 1993). Glucuronidation of the metabolites and biliary excretion was thought to be the final

elimination process for amiodarone (Freedman and Somberg, 1991). However, the phase II metabolism of amiodarone had not been comprehensively studied, although there is indirect evidence (after hydrolysis) for glucuronide metabolites of amiodarone in human plasma (Ha et al., 2005). The results from present study demonstrated that glucuronidation was the most important conjugation pathway for amiodarone and its phase I metabolites. Indeed, 11 glucuronide conjugates were identified in human bile samples. Amiodarone has a triethylamine moiety, and *N*-glucuronidation has proven to be a common metabolic pathway in the human metabolism of drugs with an aliphatic tertiary amine group (Hawes, 1998); therefore, glucuronide metabolites can have linkages of glucuronic acid through O or N atoms from amiodarone or its oxidized metabolites. Amiodarone underwent ω-oxidation to produce carboxyl acid metabolites (M4, M9 and M12), and M12 was a major metabolite on the basis of the chromatographic peak area. In addition, the corresponding glucuronide conjugates of these phase I metabolites were also detected (M13, M17, M19-1 and M19-2). These metabolites will be further investigated to unequivocally identify their structures.

In conclusion, the present study revealed that amiodarone could undergo extensive phase I and phase II metabolism in humans before excreted into bile. In addition to *N*-dealkylation, *O*-dealkylation, deamination and hydroxylation, novel metabolic pathways were proposed, including ω-carboxylation, deiodination and glucuronide conjugation. Twenty-two phase I and 11 phase II metabolites were identified in human bile, among them, 4'-carboxylamiodarone was the most abundant metabolite in humans. Further investigation is needed to understand the importance of these metabolites from both safety and efficacy perspective. This is the first time that human bile was used for the study of amiodarone metabolism. However, caution is required in extrapolating these results to patients without T-tube bile drainage because a T-tube drain may partially block enterohepatic circulation. In addition, results were obtained from a small patient sample and drug metabolism is known to vary significantly from patient to patient. Nevertheless, this study has increased our knowledge of the metabolic pathways of amiodarone in humans, and these findings underscore the importance of biliary excretion in the elimination of this drug in humans.

Acknowledgments

We thank Dr. Ke Li, Ms Cen Xie, Mr Xin Zhou and Mr Xingxing Diao for the purification of the standard compounds, and Ms Hua Li for the help during experimentation.

Authorship Contributions

Participated in research design: Deng, You, Chen, Yuan, Huang, and Zhong.

Conducted experiments: Deng, You, Yuan and Huang.

Contributed new reagents or analytic tools: Deng, Chen, Huang, and Zhong.

Performed data analysis: Deng, Chen, Yuan, Huang, and Zhong.

Wrote or contributed to the writing of the manuscript: Deng, Chen, Yuan, and Zhong.

Acquired funding fot the research: Chen.

References

Anastasiou-Nana M, Levis GM and Moulopoulos S (1982) Pharmacokinetics of amiodarone after intravenous and oral administration. *Int J Clin Pharmacol Ther Toxicol* **20:**524-529.

Berdeaux A, Roche A, Labaille T, Giroux B, Edouard A and Giudicelli JF (1984) Tissue extraction of amiodarone and N-desethylamiodarone in man after a single oral dose. *Br J Clin Pharmacol* **18:**759-763.

Bogazzi F, Bartalena L, Gasperi M, Braverman LE and Martino E (2001) The various effects of amiodarone on thyroid function. *Thyroid* **11:**511-519.

Broekhuysen J, Laruel R and Sion R (1969) [Research on the benzofuran series. XXXVII. Comparative study of transit and metabolism of amiodarone in different species of animals and humans]. *Arch Int Pharmacodyn Ther* **177:**340-359.

Chmela Z, Vesely J, Lemr K, Rypka M, Hanus J, Havlicek L, Krystof V, Michnova L, Fuksova K and Lukes J (2001) In vivo metabolism of 2,6,9-trisubstituted purine-derived cyclin-dependent kinase inhibitor bohemine in mice: glucosidation as the principal metabolic route. *Drug Metab Dispos* **29:**326-334.

Flanagan RJ, Storey GC, Holt DW and Farmer PB (1982) Identification and measurement of desethylamiodarone in blood plasma specimens from amiodarone-treated patients. *J Pharm Pharmacol* **34:**638-643.

Freedman MD and Somberg JC (1991) Pharmacology and pharmacokinetics of amiodarone. *J Clin Pharmacol* **31:**1061-1069.

Ghibellini G, Leslie EM and Brouwer KL (2006) Methods to evaluate biliary excretion of drugs in humans: an updated review. *Mol Pharm* **3:**198-211.

Ha HR, Bigler L, Binder M, Kozlik P, Stieger B, Hesse M, Altorfer HR and Follath F (2001a) Metabolism of amiodarone (part I): identification of a new hydroxylated metabolite of amiodarone. *Drug Metab Dispos* **29:**152-158.

Ha HR, Bigler L, Wendt B, Maggiorini M and Follath F (2005) Identification and quantitation of novel metabolites of amiodarone in plasma of treated patients. *Eur J Pharm Sci* **24:**271-279.

Ha HR, Candinas R, Stieger B, Meyer UA and Follath F (1996) Interaction between amiodarone and lidocaine. *J Cardiovasc Pharmacol* **28:**533-539.

Ha HR, Kozlik P, Stieger B, Bigler L and Follath F (2001b) Metabolism of amiodarone. II. High-performance liquid chromatographic assay for mono-N-desethylamiodarone hydroxylation in liver microsomes. *J Chromatogr B Biomed Sci Appl* **757:**309-315.

Harris L, Hind CR, McKenna WJ, Savage C, Krikler SJ, Storey GC and Holt DW (1983) Renal elimination of amiodarone and its desethyl metabolite. *Postgrad Med J* **59:**440-442.

Harvey DJ (1989) Further studies on the oxidative cleavage of the pentyl side-chain of cannabinoids: identification of new biotransformation pathways in the metabolism of 3'-hydroxy-delta-9-tetrahydrocannabinol by the mouse. *Xenobiotica* **19:**1437-1447.

Hawes EM (1998) N+-glucuronidation, a common pathway in human metabolism of drugs with a tertiary amine group. *Drug Metab Dispos* **26:**830-837.

Latini R, Tognoni G and Kates RE (1984) Clinical pharmacokinetics of amiodarone. *Clin Pharmacokinet* **9:**136-156.

Martino E, Bartalena L, Mariotti S, Aghini-Lombardi F, Ceccarelli C, Lippi F, Piga M, Loviselli A, Braverman L, Safran M and et al. (1988) Radioactive iodine thyroid uptake in patients with amiodarone-iodine-induced thyroid dysfunction. *Acta Endocrinol (Copenh)* **119:**167-173.

Martino E, Safran M, Aghini-Lombardi F, Rajatanavin R, Lenziardi M, Fay M, Pacchiarotti A, Aronin N, Macchia E, Haffajee C and et al. (1984) Environmental iodine intake and thyroid dysfunction during chronic amiodarone therapy. *Ann Intern Med* **101:**28-34.

Naccarelli GV, Wolbrette DL, Dell'Orfano JT, Patel HM and Luck JC (2000) Amiodarone: what have we learned from clinical trials? *Clin Cardiol* **23:**73-82.

Nassar AF, Hollenberg PF and Scatina J (2009) CYP carbon hydroxylation reaction, in: *Drug Metabolism Handbook: Concepts and Applications* (Nassar AF ed), pp 27, John Wiley & Sons, Inc, Hoboken.

Pitsiavas V, Smerdely P and Boyages SC (1999) Amiodarone compared with iodine exhibits a potent and persistent inhibitory effect on TSH-stimulated cAMP production in vitro: a possible mechanism to explain amiodarone-induced hypothyroidism. *Eur J Endocrinol* **140:**241-249.

Roden DM (1993) Pharmacokinetics of amiodarone: implications for drug therapy. *Am J Cardiol* **72:**45F-50F.

Rucker G, Neugebauer M and Zhong D (1992) Study on the metabolism of racemic prolintane and its optically pure enantiomers. *Xenobiotica* **22:**143-152.

Samara E, Bialer M, Bar-On H and Harvey DJ (1990) Identification of metabolites of the 1",1"-dimethylheptyl analogue of cannabidiol in rat and dog in vivo. *Xenobiotica* **20:**447-455.

Shiraishi K, Ko S, Sahoo SK, Muramatsu Y, Los IP, Korzun VN, Tsigankov NY and Zamostyan PV (2006) Dietary iodine intake in residents of northwestern regions of ukraine contaminated by the chernobyl accident. *Health Phys* **90:**11-15.

Sohlenius-Sternbeck AK, Chelpin HV, Orzechowski A and Halldin MM (2000) Metabolism of sameridine to monocarboxylated products by hepatocytes isolated from the male rat. *Drug Metab Dispos* **28:**695-700.

Storey GC, Adams PC, Campbell RW and Holt DW (1983) High-performance liquid chromatographic measurement of amiodarone and desethylamiodarone in small tissue samples after enzymatic digestion. *J Clin Pathol* **36:**785-789.

Walsh JS, Reese MJ and Thurmond LM (2002) The metabolic activation of abacavir by human liver cytosol and expressed human alcohol dehydrogenase isozymes. *Chem Biol Interact* **142:**135-154.

Young RA and Mehendale HM (1986) In vitro metabolism of amiodarone by rabbit and rat liver and small intestine. *Drug Metab Dispos* **14:**423-429.

Footnote

This work was supported by the National Science and Technology Major Project “Key New Drug Creation and Manufacturing Program”, China [Grant 2009ZX09301-001].

Legends for figures

Fig. 1. Mass spectrum of amiodarone obtained on Q-TOF mass spectrometry at high collision energy (A), and tentative structures of the most informative fragment ions for amiodarone (B). The structure of amiodarone could be divided into three parts according to the fragment pattern.

Fig. 2. Metabolite profiles of amiodarone in human bile after once daily oral administration of 200 mg amiodarone hydrochloride for 7 days (A), and extracted ion chromatograms of amiodarone metabolites M8 (B), M11 (C) and M18 (D).

Fig. 3. Proposed metabolic pathways of amiodarone in humans.

Fig. 4. Key HMBC correlations of 3'-hydroxylamiodarone. The long-range coupling between H_3-4', H_2-1' and H_2-2' to C-3', and from H-3' to C-1', C-2' and C-4' were observed, which confirms the attachment of a hydroxyl group to C-3'.

Fig. 5. ^{1}H NMR spectrum of amiodarone (A) and 4'-carboxylamiodarone (B).

Fig. 6. In vitro metabolism of amiodarone (50 μM) mediated by human liver microsomes (1.0 mg/ml). UPLC-Q/TOF MS chromatogram of a control incubation performed in the absence of NADPH (A); UPLC-Q/TOF MS chromatogram of an incubation performed in the presence of NADPH (B); UPLC-UV chromatogram of an incubation performed in the presence of NADPH (C) (insert is the expanded chromatogram in the region of 11-17 min).

Fig. 7. In vitro metabolism of amiodarone (50 μM) mediated by human liver S9 (2.0 mg/ml). UPLC-Q/TOF MS chromatogram of a control incubation performed in the absence of NADPH (A); UPLC-Q/TOF MS chromatogram of an incubation performed in the presence of NADPH (B); UPLC-UV chromatogram of an incubation performed in the presence of NADPH (C) (insert is the expanded chromatogram in the region of 11-17 min).

Tables

Table 1. Identification of amiodarone metabolites in human bile after oral drug administration using UPLC-Q/TOF mass spectrometry.

	Description	Retention Time (min)	Formula	Measured Mass $[M + H]^+$	Calculated Mass $[M + H]^+$	Fragment Ions
M0	Parent	18.0	$C_{25}H_{29}I_2NO_3$	646.029	646.032	372.831, 276.082, 247.078, 245.956, 217.926, 201.094, 119.021, 100.113
M1	*N*-Desethylation – I + H	16.2	$C_{23}H_{26}INO_3$	492.108	492.104	
M2	*N*-Desethylation + Hydroxylation – I + H	13.1	$C_{23}H_{26}INO_4$	508.097	508.099	437.024, 419.017
M3	Parent – $C_6H_{13}N$	16.3	$C_{19}H1_6I_2O_3$	546.925	546.927	372.858
M4	4'-Carboxylamiodarone – I + H	13.3	$C_{25}H_{28}INO_5$	550.109	550.109	276.070, 100.113
M5	Hydroxylation – C_4H_9N	21.5	$C_{21}H_{20}I_2O_4$	590.952	590.953	546.930, 372.818, 217.927, 201.091, 119.013, 91.018
M6-1	2 × Hydroxylation – C_4H_9N	14.4	$C_{21}H_{20}I_2O_5$	606.943	606.948	562.924, 544.915, 372.830
M6-2	2 × Hydroxylation – C_4H_9N	18.6	$C_{21}H_{20}I_2O_5$	606.943	606.948	562.925, 544.917, 372.828
M7	*N*-Desethylation	17.0	$C_{23}H_{25}I_2NO_3$	617.996	618.000	372.858, 201.090
M8-1	*N*-Desethylation + Hydroxylation	13.5	$C_{23}H_{25}I_2NO_4$	633.989	633.995	372.820
M8-2	*N*-Desethylation + Hydroxylation	13.7	$C_{23}H_{25}I_2NO_4$	633.992	633.995	372.821, 562.922, 544.908
M8-3	*N*-Desethylation + Hydroxylation	14.0	$C_{23}H_{25}I_2NO_4$	633.994	633.995	372.822, 562.923, 544.908
M8-4	*N*-Desethylation + Hydroxylation	14.4	$C_{23}H_{25}I_2NO_4$	633.997	633.995	372.821, 562.922, 544.907
M8-5	*N*-Desethylation + Hydroxylation	14.7	$C_{23}H_{25}I_2NO_4$	633.990	633.995	372.824
M9	4'-Carboxylamiodarone + *N*-Desethylation	13.4	$C_{23}H_{23}I_2NO_5$	647.975	647.974	
M10-1	*N*-Desethylation + Dihydroxylation	11.6	$C_{23}H_{25}I_2NO_5$	649.985	649.990	372.823, 245.923, 217.928, 119.016, 91.020
M10-2	*N*-Desethylation + Dihydroxylation	12.0	$C_{23}H_{25}I_2NO_5$	649.988	649.990	372.822, 245.925, 217.922, 119.013, 91.021

M11-1	4'-Hydroxylation	14.3	$C_{25}H_{29}I_2NO_4$	662.026	662.026	372.858, 100.113
M11-2	3'-Hydroxylation	14.5	$C_{25}H_{29}I_2NO_4$	662.024	662.026	372.824, 100.114
M11-3	Hydroxylation	14.9	$C_{25}H_{29}I_2NO_4$	662.024	662.026	
M11-4	Hydroxylation	15.3	$C_{25}H_{29}I_2NO_4$	662.025	662.026	
M11-5	2-Hydroxylation	15.5	$C_{25}H_{29}I_2NO_4$	662.023	662.026	372.822, 100.114
M12	4'-Carboxylamiodarone	14.2	$C_{25}H_{27}I_2NO_5$	676.002	676.006	372.823, 245.926, 217.925, 100.122
M13	4'-Carboxylamiodarone + Glucuronidation – I + H	11.9	$C_{31}H_{36}INO_{11}$	726.139	726.141	550.112
M14	Hydroxylation + Glucuronidation - C_4H_9N	18.1	$C_{27}H_{28}I_2O_{10}$	766.987	766.985	590.954, 546.930
M15-1	*N*-Desethylation + Hydroxylation + Glucuronidation	12.2	$C_{29}H_{33}I_2NO_{10}$	810.028	810.027	633.998, 562.931, 544.912
M15-2	*N*-Desethylation + Hydroxylation + Glucuronidation	19.6	$C_{29}H_{33}I_2NO_{10}$	810.027	810.027	633.997, 372.824
M16	*N*-Glucuronidation	16.3	$C_{31}H_{37}I_2NO_9$	822.061	822.064	646.024
M17	*N*-Desethylation + 4'-Carboxylamiodarone + Glucuronidation	12.1	$C_{29}H_{31}I_2NO_{11}$	824.012	824.007	647.980
M18-1	Hydroxylation + Glucuronidation	12.6	$C_{31}H_{37}I_2NO_{10}$	838.050	838.059	662.027, 372.825, 100.113
M18-2	Hydroxylation + Glucuronidation	12.8	$C_{31}H_{37}I_2NO_{10}$	838.059	838.059	662.025, 372.823, 100.114
M18-3	Hydroxylation + Glucuronidation	13.0	$C_{31}H_{37}I_2NO_{10}$	838.060	838.059	662.028, 372.822, 100.115
M19-1	4'-Carboxylamiodarone + Glucuronidation	12.4	$C_{31}H_{35}I_2NO_{11}$	852.035	852.038	676.009
M19-2	4'-Carboxylamiodarone + Glucuronidation	12.9	$C_{31}H_{35}I_2NO_{11}$	852.044	852.038	676.008

DMD Fast Forward. Published on March 11, 2011 as DOI: 10.1124/dmd.110.037671
This article has not been copyedited and formatted. The final version may differ from this version.

Table 2. ^{1}H NMR spectra data of amiodarone, 4'-carboxylamiodarone, 2-hydroxylamiodarone and 3'-hydroxylamiodarone.

No.	Proton signals			
	Amiodarone	4′-Carboxylamiodarone	2-Hydroxylamiodarone	3′-Hydroxylamiodarone
1	7.42 (d, *J* = 7.8 Hz)	7.39 (d, *J* = 7.7 Hz)	6.94 (d, *J* = 1.7 Hz)	7.53 (d, *J* = 7.8 Hz)
2	7.33 (t, *J* = 7.7 Hz)	7.34 (t, *J* = 7.7 Hz)		7.33 (d, *J* = 7.8 Hz)
3	7.24 (t, *J* = 7.5 Hz)	7.25 (t, *J* = 7.6 Hz)	6.78 (dd, *J* = 8.5, 1.7 Hz)	7.24 (d, *J* = 7.8 Hz)
4	7.52 (d, *J* = 7.8 Hz)	7.54 (d, *J* = 8.1 Hz)	7.23 (d, *J* = 8.5 Hz)	7.38 (d, *J* = 7.8 Hz)
9, 13	8.18 (s)	8.21 (s)	8.21 (s)	8.19 (s)
14	4.19 (t, *J* = 6.4 Hz, 2H)	4.29 (t, *J* = 6.1 Hz, 2H)	4.29 (t, *J* = 6.0 Hz, 2H)	4.18 (t, *J* = 6.1 Hz, 2H)
15	3.15 (t, *J* = 6.4 Hz, 2H)	3.36 (t, *J* = 6.1 Hz, 2H)	3.18 (t, *J* = 6.0 Hz, 2H)	3.14 (t, *J* = 6.1 Hz, 2H)
16, 18	2.79 (q, *J* = 7.1 Hz, 4H)	3.04 (q, *J* = 6.9 Hz, 4H)	3.02 (q, *J* = 7.0 Hz, 4H)	2.78 (q, *J* = 7.1 Hz, 4H)
17, 19	1.16 (t, *J* = 7.1 Hz, 6H)	1.25 (t, *J* = 6.9 Hz, 6H)	1.26 (t, *J* = 7.0 Hz, 4H)	1.14 (t, *J* = 7.1 Hz, 6H)
1′	2.81 (t, *J* = 7.2 Hz, 2H)	2.91 (t, *J* = 7.3 Hz, 2H)	2.79 (m, 2H)	2.94 (m, 2H)
2′	1.76 (m, 2H)	2.06 (m, 2H)	1.91 (m, 2H)	1.88 (m, 2H)
3′	1.35 (m, 2H)	2.21 (m, 2H)	1.42 (m, 2H)	3.69 (m, 1H)
4′	0.92 (t, *J* = 7.3 Hz, 3H)		0.95 (t, *J* = 7.0 Hz, 3H)	1.15 (d, *J* = 7.2 Hz, 3H)

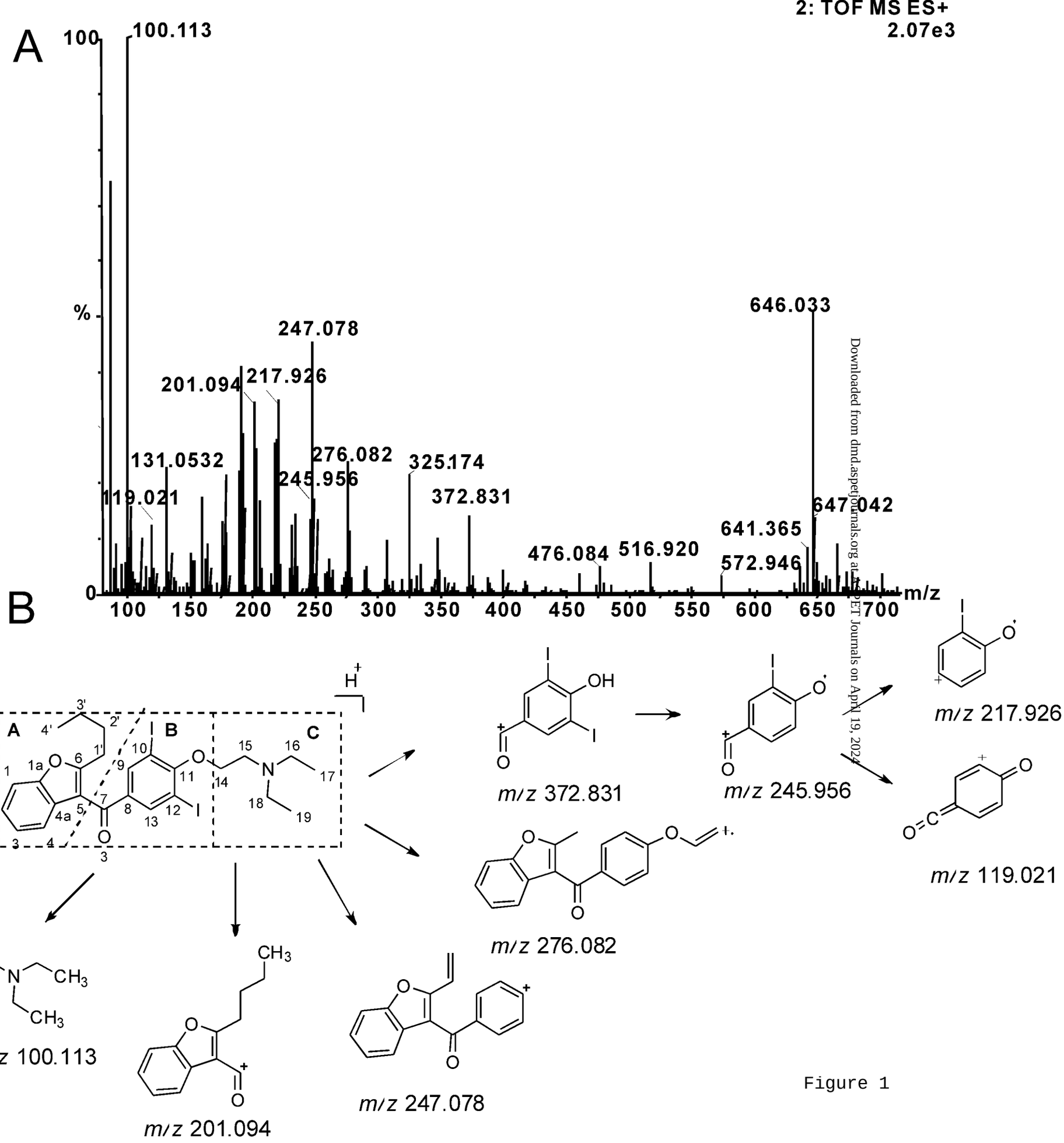

Figure 1

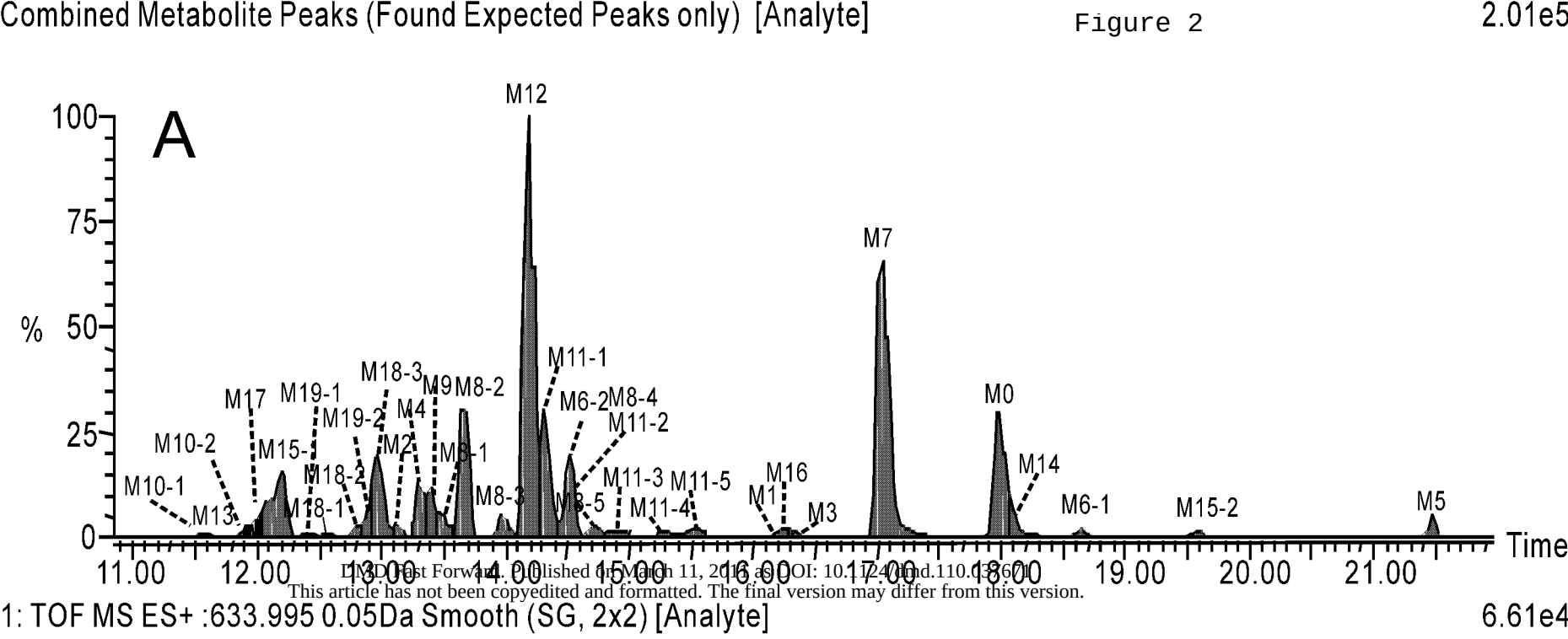

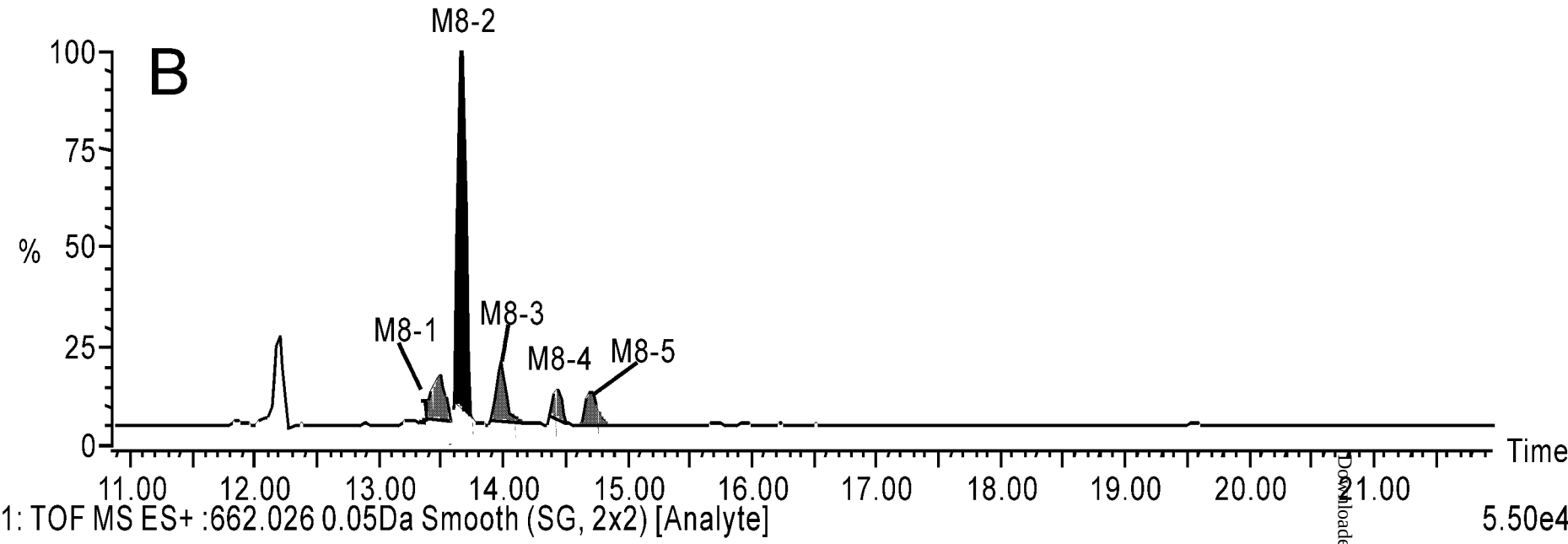

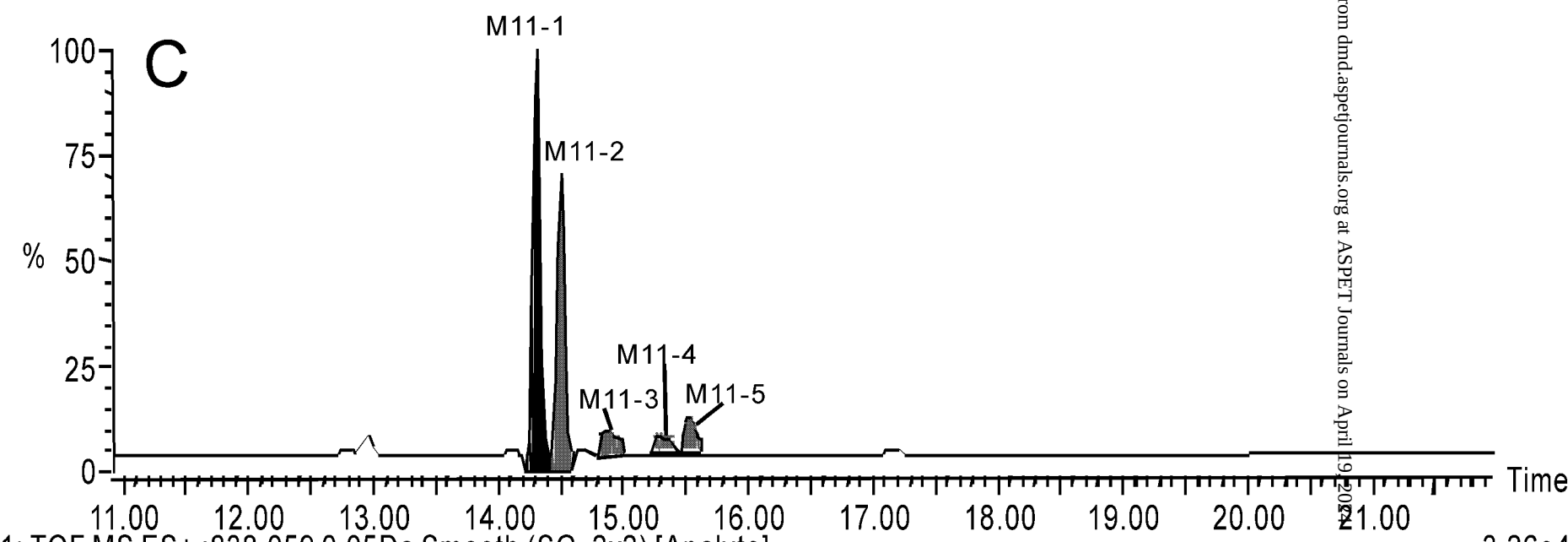

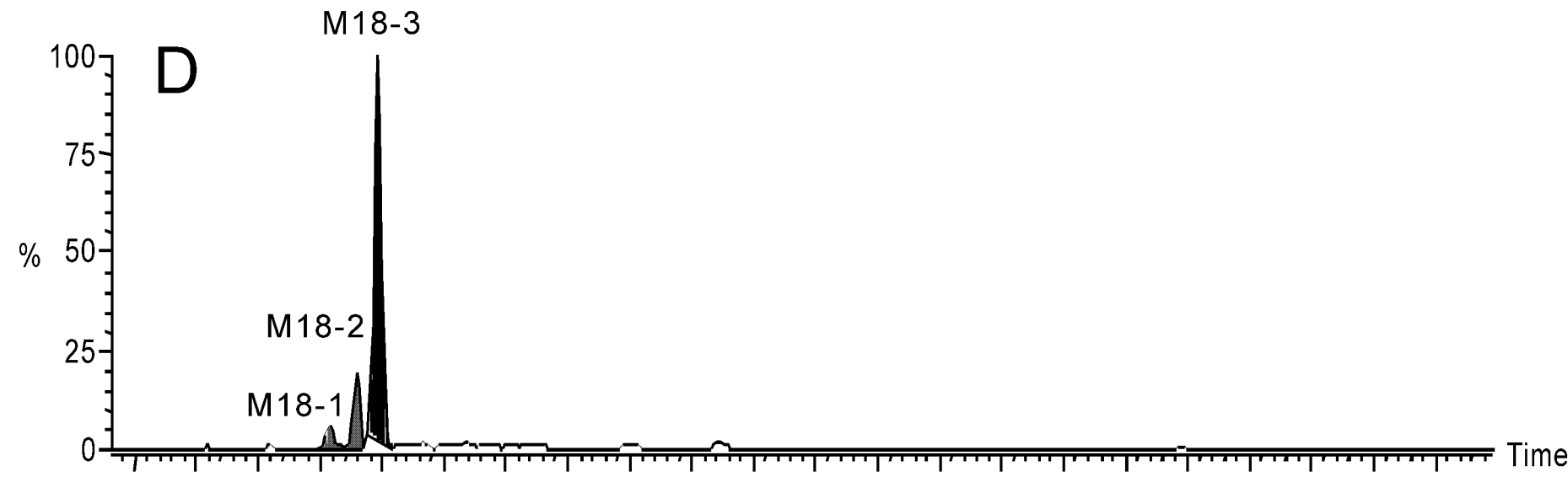

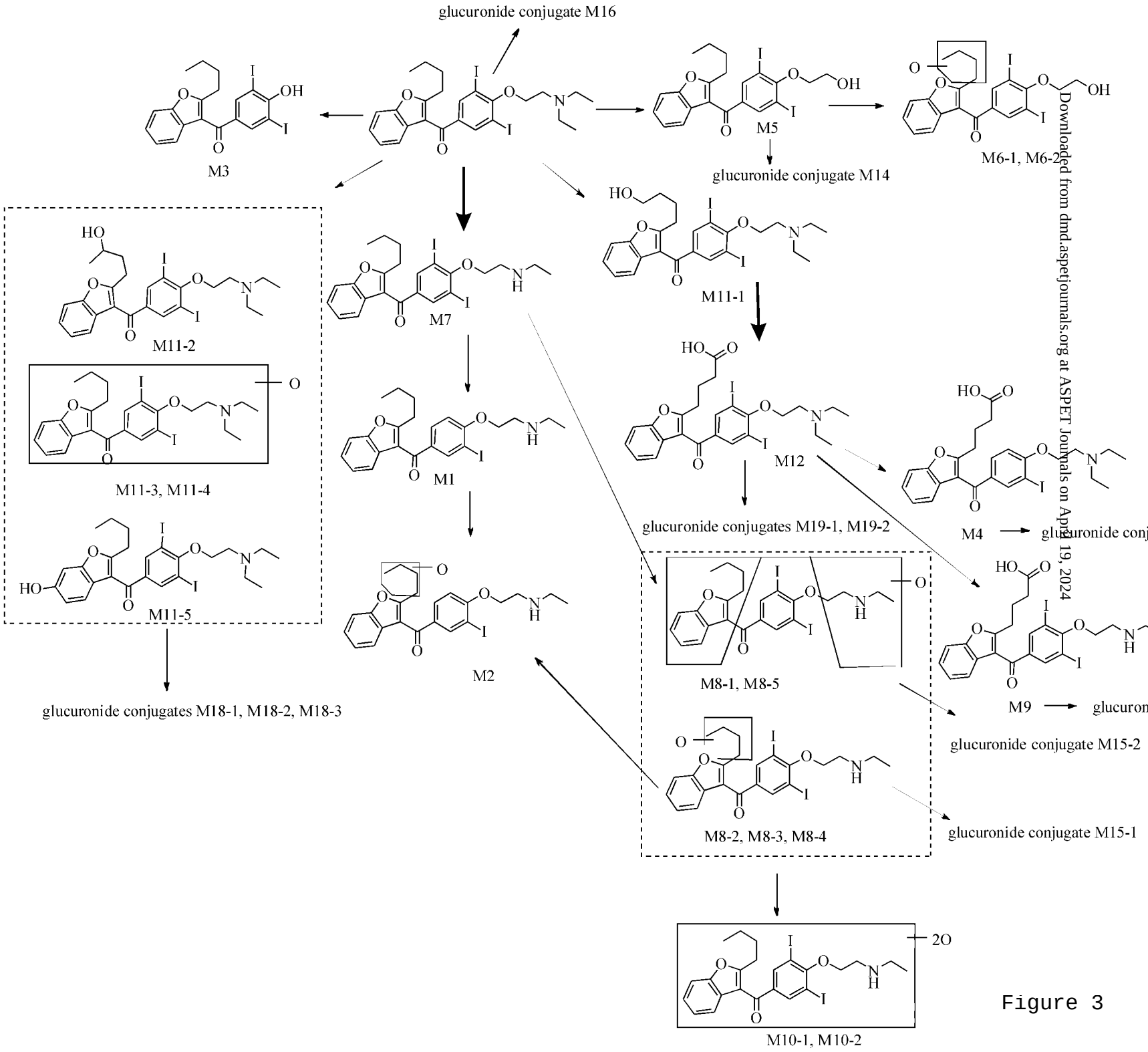

Figure 3

Figure 4

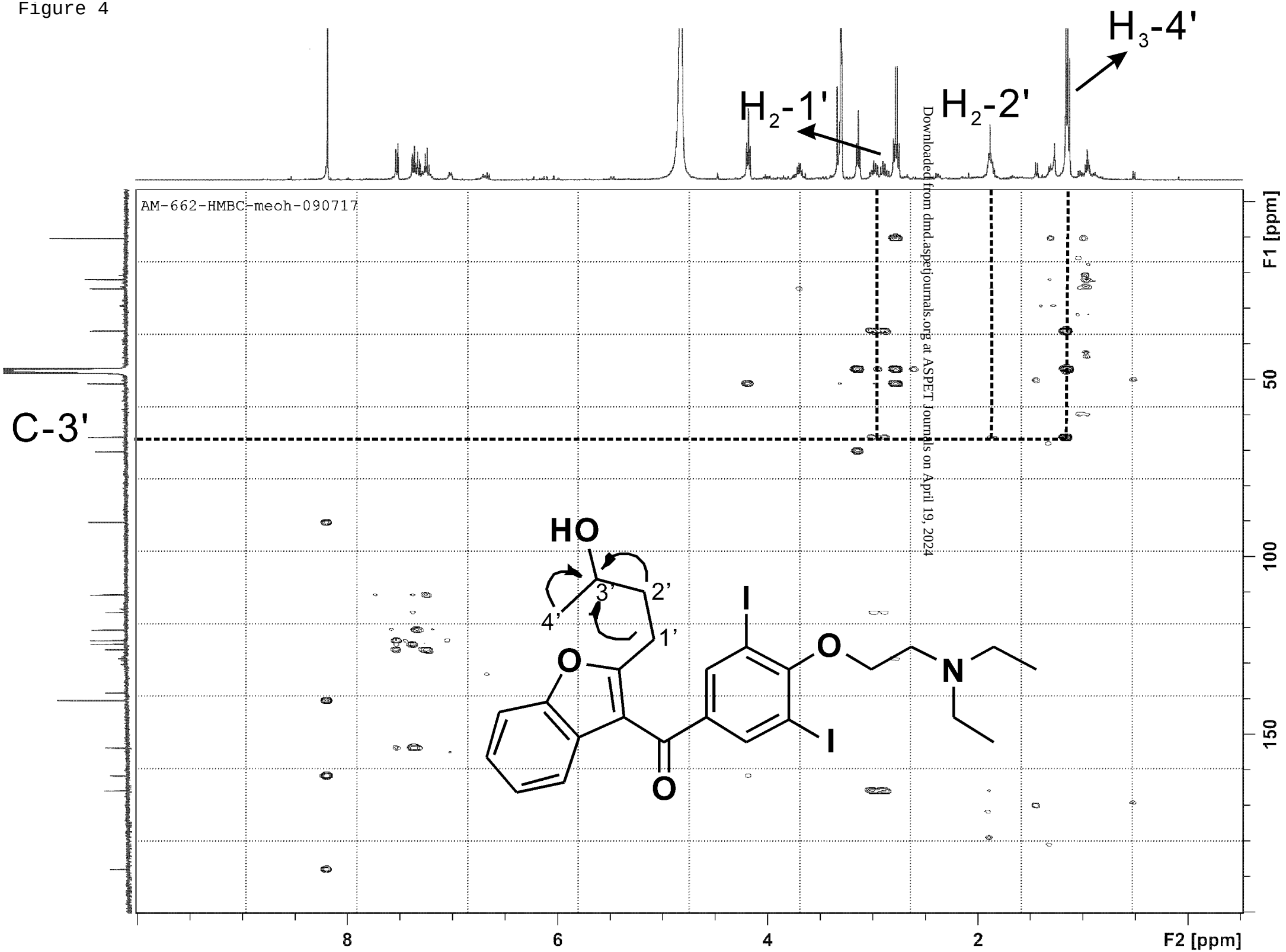

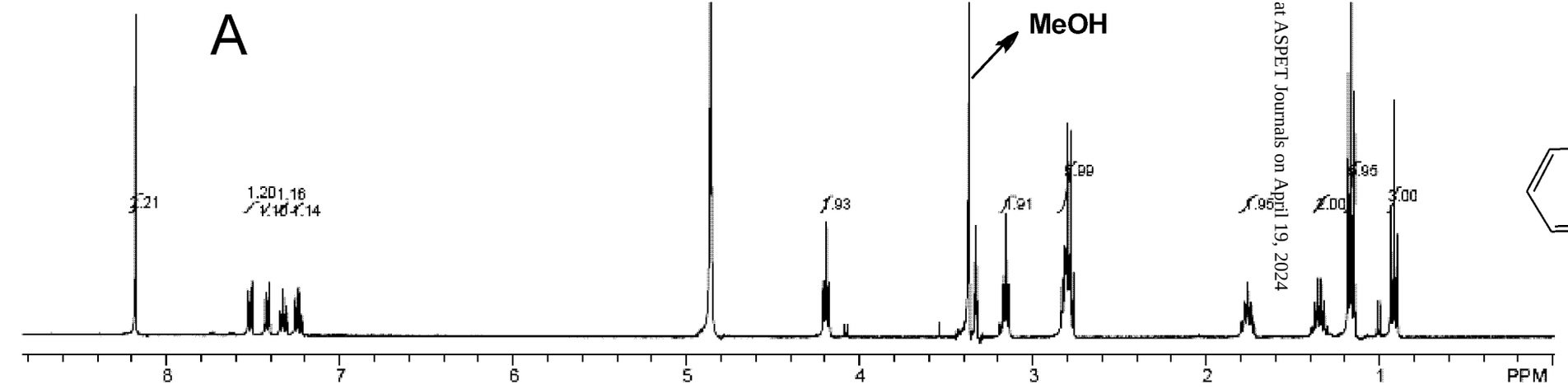

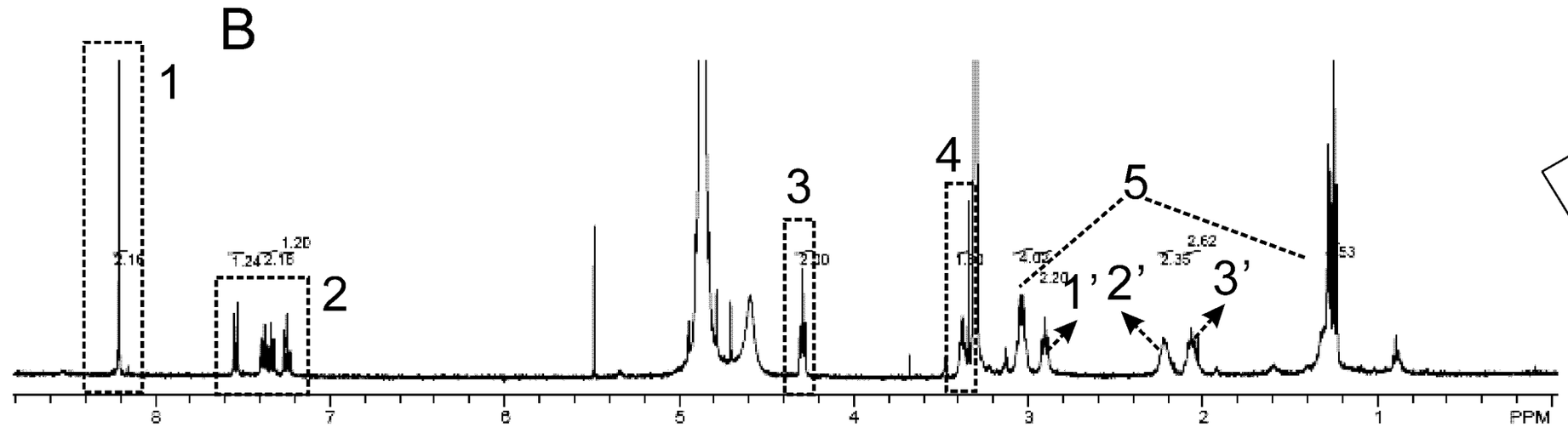

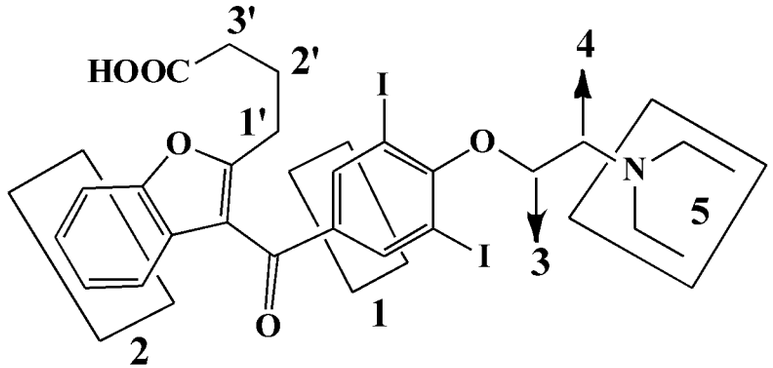

Figure 5

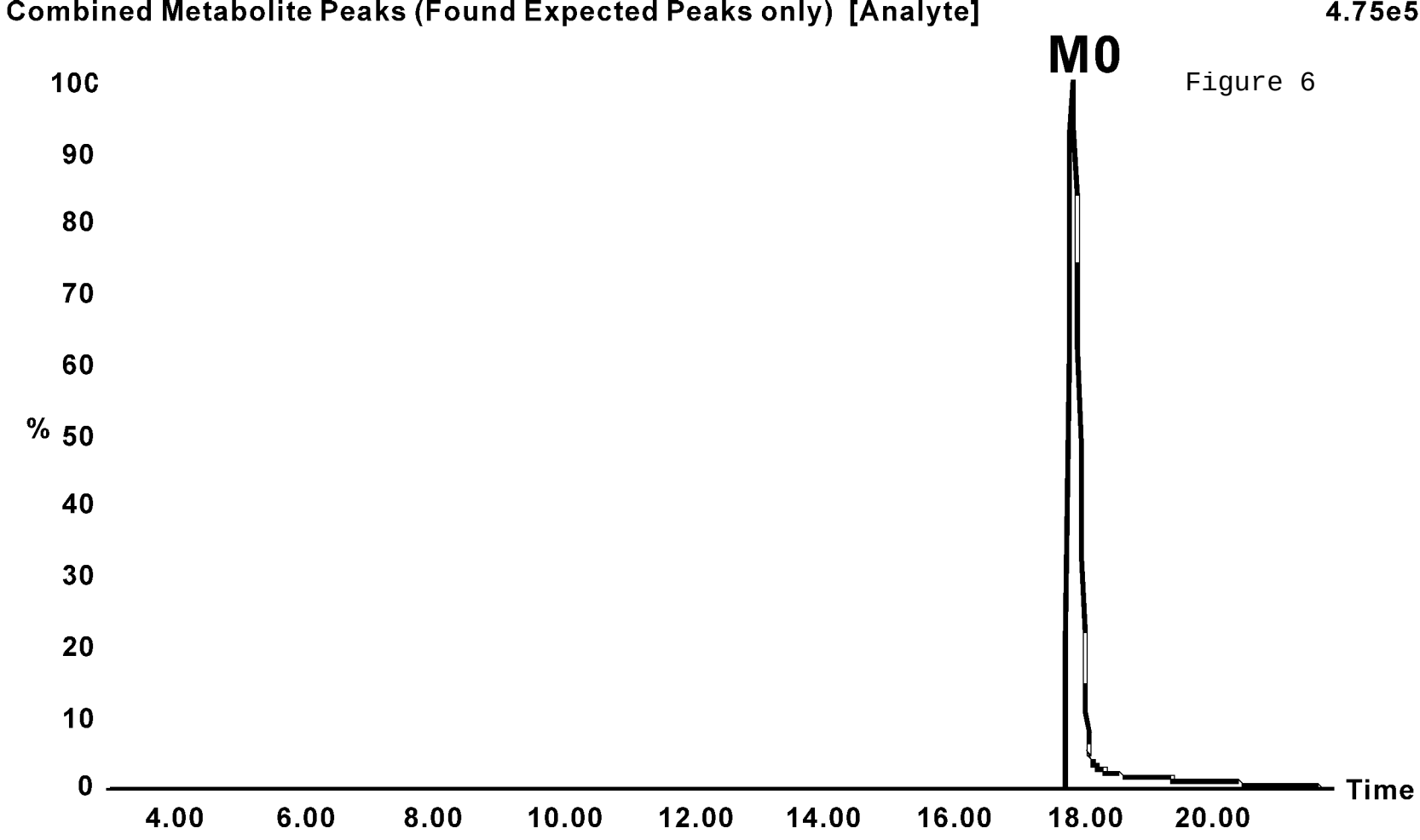

DMD Fast Forward. Published on March 11, 2011 as DOI: 10.1124/dmd.110.037671
This article has not been copyedited and formatted. The final version may differ from this version.